Int J Fract (2007) 146:125–138
DOI 10.1007/s10704-007-9150-x

ORIGINAL PAPER

Fracture analysis of a penny-shaped magnetically dielectric crack in a magnetoelectroelastic material

W. J. Feng · R. K. L. Su · E. Pan

Received: 19 January 2007 / Accepted: 12 October 2007 / Published online: 2 November 2007

Abstract In this paper we investigate the magnetoelectroelastic behavior induced by a penny-shaped crack in a magnetoelectroelastic material. The crack is assumed to be *magnetically dielectric*. A closed-form solution is derived by virtue of Hankel transform technique with the introduction of certain auxiliary functions. Field intensity factors are obtained and analyzed. The results indicate that the stress intensity factor depends only on the mechanical loads. However, all the other field intensity factors depend directly on both the magnetic and dielectric permeabilities inside the crack as well as on the applied magnetoelectromechanical loads and the material properties of the magnetoelectroelastic material. Several special cases are further discussed, with the reduced results being in agreement with those from literature. Finally, according to the maximum crack opening displacement (COD) criterion, the effects of the magnetoelectromechanical loads and the crack surface conditions on the crack propagation and growth are evaluated.

W. J. Feng
Department of Engineering Mechanics, Shijiazhuang Railway Institute, Shijiazhuang 050043, P.R. China

R. K. L. Su (✉)
Department of Civil Engineering, The University of Hong Kong, Hong Kong, P.R. China
e-mail: klsu@hkucc.hku.hk

E. Pan
Department of Civil Engineering, The University of Akron, Akron, OH 44325, USA

Keywords Magnetically dielectric crack · Penny-shaped crack · Field intensity factor · COD fracture criterion · Magnetoelectroelastic behavior · Magnetoelectroelastic materials · Hankel transform

1 Introduction

Materials possessing magnetoelectroelastic coupling effects have found increasing applications in engineering structures, particularly in smart materials/intelligent structures. The effects of magnetoelectromechanical coupling have been observed in single-phase materials where simultaneous magnetic and electric order coexists, and in two-phase composites where the participating phases are piezoelectric and piezomagnetic (Avellaneda and Harshe 1994; Benvensite 1995; Harshe et al. 1993; Huang and Kuo 1997; Kirchner and Alshits 1996; Li and Dunn 1998; Nan 1994). In recent years, an area of increasing interest is the fracture mechanics of magnetoelectroelastic materials, which combine the ferromagnetic and ferroelectric phases (Liu et al. 2001; Song and Sih 2003; Gao et al. 2003; Gao and Noda 2004; Wang and Mai 2004, 2007; Zhou et al. 2004; Hu and Li 2005; Tian and Gabbert 2005; Chue and Liu 2005; Feng et al. 2005; Hu et al. 2006; Li and Kardomateas 2006; Niraula and Wang 2006; Feng and Su 2006), where magnetoelectrically impermeable and/or permeable crack surface assumptions are applied. The reason of making the assumptions is perhaps that one can directly extend the two kinds of

idealized electrical boundary condition of the crack-faces, i.e., electrically impermeable crack (Pak 1990) and permeable crack (Parton 1976) used for piezoelectric ceramics to magnetoelectroelastic materials.

However, for piezoelectric ceramics, exact analyzes of electroelastic fields for a slender hole (Dunn 1994; Sosa and Khutoryansky 1996; Zhang et al. 1998; Gao and Fan 1999) show that the electrically impermeable assumption could introduce significant errors in determining electroelastic behavior, since the dielectric permittivity of the crack interior is, in fact, present, even though it is small. On the other hand, for an electrically permeable crack, because the dielectric permittivity of the opening crack interior, in fact, does not enter the electric boundary conditions, the effects of the dielectric of the opening crack interior are still neglected, although an ideal crack has a zero separation between two crack surfaces before crack opening. Therefore, electrically permeable assumption also causes errors in some extent. Hao and Shen (1994) proposed the following expressions between the electric field and electric displacement inside an opening crack

$$E^{(c)} = -\frac{\Delta\phi}{\Delta u_z}, \quad D^{(c)} = -\varepsilon^{(c)}\frac{\Delta\phi}{\Delta u_z}, \tag{1}$$

where $\Delta\phi$ and Δu_z denote the voltage and the crack opening displacement (COD), $\varepsilon^{(c)}$ denotes the permittivity of the crack interior. The crack surface assumption is referred to the exact electric boundary condition and the corresponding crack is called a dielectric crack. The advantage of the exact electric boundary condition over the impermeable and permeable conditions has been shown by the finite-element analysis (McMeeking 1999). In the last few years, the electroelastic behavior induced by a dielectric crack embedded in piezoelectric materials were widely investigated for two-dimensional crack problems (McMeeking 2001; Xu and Rajapakse 2001; Wang and Jiang 2002, 2004; Zhang et al. 2002; Wang and Mai 2003) and for three-dimensional penny-shaped crack problems (Li and Lee 2004).

For crack problems of magnetoelectroelastic materials, the crack-face magnetoelectric boundary conditions ought to be one of the basic and important issues on fracture analyzes. However, as pointed out before, in most of these studies, the crack model was assumed to be either magnetoelectrically impermeable or permeable. Based on the results of piezoelectric ceramics, these assumptions will probably cause some errors in a certain extent.

In addition, for the three-dimensional crack analysis, although some achievements for piezoelectric ceramics are made (Wang 1992; Jiang and Sun 2001; Kogan et al. 1996; Chen and Shioya 1999; Karapetian et al. 2000; Yang and Lee 2002, 2003; Li and Lee 2004), to the best of the authors' knowledge, only few results related to the fracture behaviors of a crack in a three-dimensional magnetoelectroelastic body have been reported (Niraula and Wang 2006; Zhao et al. 2006; Feng et al. 2007). Among these studies, Niraula and Wang (2006) derived an exact closed-form solution for a penny-shaped crack in a magnetoelectrothermoelastic material in a temperature field. Zhao et al. (2006) obtained the solution for an ellipsoidal cavity in an infinite transversely isotropic magnetoelectroelastic medium and derived the exact solution for a penny-shaped crack by setting the minor axis of the cavity approaching zero. Feng et al. (2007) considered the dynamic fracture problems of a penny-shaped crack in a finite magnetoelectroelastic layer. It should be pointed out that in the work of both Niraula and Wang (2006) and Feng et al. (2007), the crack surfaces are assumed to be magnetoelectrically impermeable or permeable.

In this paper, based on the more accurate crack surface conditions, a magnetically dielectric penny-shaped crack embedded in a magnetoelectroelastic space is considered. Different from Zhao et al. (2006), a closed-form solution is directly derived by means of the Hankel transform technique. The field intensity factors are also obtained and discussed in detail. Some numerical results of COD intensity factor are presented to predict crack propagation and growth.

2 Statement of the problem

Consider a class of axisymmetric problems of a transversely isotropic magnetoelectroelastic material with the poling direction as the z-axis and the isotropic plane as the xy-plane. The constitutive equations within the framework of the theory of linear magnetoelectroelastic medium take the form (Feng et al. 2007)

$$\begin{Bmatrix} \sigma_{rr} \\ \sigma_{\theta\theta} \\ \sigma_{zz} \\ \sigma_{rz} \end{Bmatrix} = \begin{bmatrix} c_{11} & c_{12} & c_{13} & 0 \\ c_{12} & c_{11} & c_{13} & 0 \\ c_{13} & c_{13} & c_{33} & 0 \\ 0 & 0 & 0 & c_{44} \end{bmatrix} \begin{Bmatrix} \frac{\partial u_r}{\partial r} \\ \frac{u_r}{r} \\ \frac{\partial u_z}{\partial z} \\ \frac{\partial u_r}{\partial z} + \frac{\partial u_z}{\partial r} \end{Bmatrix}$$

$$+\begin{bmatrix} 0 & e_{31} \\ 0 & e_{31} \\ 0 & e_{33} \\ e_{15} & 0 \end{bmatrix} \begin{Bmatrix} \frac{\partial \phi}{\partial r} \\ \frac{\partial \phi}{\partial z} \end{Bmatrix} + \begin{bmatrix} 0 & f_{31} \\ 0 & f_{31} \\ 0 & f_{33} \\ f_{15} & 0 \end{bmatrix} \times \begin{Bmatrix} \frac{\partial \psi}{\partial r} \\ \frac{\partial \psi}{\partial z} \end{Bmatrix}, \tag{2a}$$

$$\begin{Bmatrix} D_r \\ D_z \end{Bmatrix} = \begin{bmatrix} 0 & 0 & 0 & e_{15} \\ e_{31} & e_{31} & e_{33} & 0 \end{bmatrix} \begin{Bmatrix} \frac{\partial u_r}{\partial r} \\ \frac{u_r}{r} \\ \frac{\partial u_z}{\partial z} \\ \frac{\partial u_r}{\partial z} + \frac{\partial u_z}{\partial r} \end{Bmatrix} - \begin{bmatrix} \varepsilon_{11} & 0 \\ 0 & \varepsilon_{33} \end{bmatrix} \begin{Bmatrix} \frac{\partial \phi}{\partial r} \\ \frac{\partial \phi}{\partial z} \end{Bmatrix} - \begin{bmatrix} g_{11} & 0 \\ 0 & g_{33} \end{bmatrix} \times \begin{Bmatrix} \frac{\partial \psi}{\partial r} \\ \frac{\partial \psi}{\partial z} \end{Bmatrix}, \tag{2b}$$

$$\begin{Bmatrix} B_r \\ B_z \end{Bmatrix} = \begin{bmatrix} 0 & 0 & 0 & f_{15} \\ f_{31} & f_{31} & f_{33} & 0 \end{bmatrix} \begin{Bmatrix} \frac{\partial u_r}{\partial r} \\ \frac{u_r}{r} \\ \frac{\partial u_z}{\partial z} \\ \frac{\partial u_r}{\partial z} + \frac{\partial u_z}{\partial r} \end{Bmatrix} - \begin{bmatrix} g_{11} & 0 \\ 0 & g_{33} \end{bmatrix} \begin{Bmatrix} \frac{\partial \phi}{\partial r} \\ \frac{\partial \phi}{\partial z} \end{Bmatrix} - \begin{bmatrix} \mu_{11} & 0 \\ 0 & \mu_{33} \end{bmatrix} \times \begin{Bmatrix} \frac{\partial \psi}{\partial r} \\ \frac{\partial \psi}{\partial z} \end{Bmatrix}, \tag{2c}$$

where corresponding components are functions of r and z, independent of angle θ. u_r and u_z are radial and axial components of the elastic displacements, respectively; ϕ and ψ are electric and magnetic potentials, respectively; σ, D, and B are stress, electric displacement and magnetic induction, respectively; c_{ij}, e_{ij}, f_{ij}, and g_{ij} are elastic, piezoelectric, piezomagnetic, and magnetoelectric constants, respectively; ε_{ij} and μ_{ij} are dielectric permittivities and magnetic permeabilities, respectively.

In the absence of body forces, free charges and electric current density, stresses, electric displacements and magnetic inductions satisfy the following equilibrium equations:

$$\frac{\partial \sigma_{rr}}{\partial r} + \frac{\partial \sigma_{rz}}{\partial z} + \frac{\sigma_{rr} - \sigma_{\theta\theta}}{r} = 0, \tag{3a}$$

$$\frac{\partial \sigma_{rz}}{\partial r} + \frac{\partial \sigma_{zz}}{\partial z} + \frac{\sigma_{rz}}{r} = 0, \tag{3b}$$

$$\frac{\partial D_r}{\partial r} + \frac{\partial D_z}{\partial z} + \frac{D_r}{r} = 0, \tag{3c}$$

$$\frac{\partial B_r}{\partial r} + \frac{\partial B_z}{\partial z} + \frac{B_r}{r} = 0. \tag{3d}$$

Substituting the constitutive equations into the above equations yields the basic governing equations for elastic displacements, u_r and u_z, electric potential ϕ, and magnetic potential ψ as follows

$$c_{11}\left(\frac{\partial^2 u_r}{\partial r^2} + \frac{1}{r}\frac{\partial u_r}{\partial r} - \frac{u_r}{r^2}\right) + c_{44}\frac{\partial^2 u_r}{\partial z^2} + (c_{13} + c_{44})\frac{\partial^2 u_z}{\partial r \partial z} + (e_{31} + e_{15})\frac{\partial^2 \phi}{\partial r \partial z} + (f_{31} + f_{15})\frac{\partial^2 \psi}{\partial r \partial z} = 0, \tag{4a}$$

$$c_{44}\left(\frac{\partial^2 u_z}{\partial r^2} + \frac{1}{r}\frac{\partial u_z}{\partial r}\right) + c_{33}\frac{\partial^2 u_z}{\partial z^2} + (c_{13} + c_{44})\left(\frac{\partial^2 u_r}{\partial r \partial z} + \frac{1}{r}\frac{\partial u_r}{\partial z}\right) + e_{15}\left(\frac{\partial^2 \phi}{\partial r^2} + \frac{1}{r}\frac{\partial \phi}{\partial r}\right) + e_{33}\frac{\partial^2 \phi}{\partial z^2} + f_{15}\left(\frac{\partial^2 \psi}{\partial r^2} + \frac{1}{r}\frac{\partial \psi}{\partial r}\right) + f_{33}\frac{\partial^2 \psi}{\partial z^2} = 0, \tag{4b}$$

$$(e_{31} + e_{15})\left(\frac{\partial^2 u_r}{\partial r \partial z} + \frac{1}{r}\frac{\partial u_r}{\partial z}\right) + e_{15}\left(\frac{\partial^2 u_z}{\partial r^2} + \frac{1}{r}\frac{\partial u_z}{\partial r}\right) + e_{33}\frac{\partial^2 u_z}{\partial z^2} - \varepsilon_{11}\left(\frac{\partial^2 \phi}{\partial r^2} + \frac{1}{r}\frac{\partial \phi}{\partial r}\right) - \varepsilon_{33}\frac{\partial^2 \phi}{\partial z^2} - g_{11}\left(\frac{\partial^2 \psi}{\partial r^2} + \frac{1}{r}\frac{\partial \psi}{\partial r}\right) - g_{33}\frac{\partial^2 \psi}{\partial z^2} = 0, \tag{4c}$$

$$(f_{31} + f_{15})\left(\frac{\partial^2 u_r}{\partial r \partial z} + \frac{1}{r}\frac{\partial u_r}{\partial z}\right) + f_{15}\left(\frac{\partial^2 u_z}{\partial r^2} + \frac{1}{r}\frac{\partial u_z}{\partial r}\right) + f_{33}\frac{\partial^2 u_z}{\partial z^2} - g_{11}\left(\frac{\partial^2 \phi}{\partial r^2} + \frac{1}{r}\frac{\partial \phi}{\partial r}\right) - g_{33}\frac{\partial^2 \phi}{\partial z^2} - \mu_{11}\left(\frac{\partial^2 \psi}{\partial r^2} + \frac{1}{r}\frac{\partial \psi}{\partial r}\right) - \mu_{33}\frac{\partial^2 \psi}{\partial z^2} = 0. \tag{4d}$$

As shown in Fig. 1, a flat penny-shaped crack of radius a perpendicular to the poling axis is situated in a magnetoelectroelastic body and occupies the region $r \le a$, $z = 0$. Suppose that the crack opens under the applied magnetoelectromechanical loads. For simplicity, only one kind of loading cases is considered, i.e.,

$$\sigma_{zz}(r, \pm\infty) = \sigma_0, \quad \sigma_{zr}(r, \pm\infty) = 0,$$
$$E_z(r, \pm\infty) = E_0, \quad H_z(r, \pm\infty) = H_0, \tag{5}$$

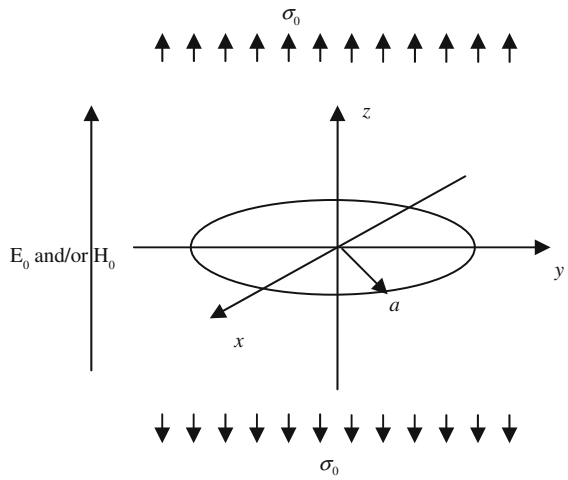

Fig. 1 Geometry of a magnetoelectroelastic material with a penny-shaped crack along with the corresponding coordinates

where σ_0, E_0, and H_0 are given constants representing the stress, electric field, and magnetic field applied at infinity, respectively. At the crack plane, elastic, electric and magnetic boundary conditions are given as follows

$$\sigma_{zz}(r,0)=0,\quad \sigma_{zr}(r,0)=0,\quad D_z(r,0)=D^{(c)},$$
$$B_z(r,0)=B^{(c)},\quad r<a, \tag{6}$$

where $B^{(c)}$ is the normal component of magnetic induction inside the crack, which is given as

$$B^{(c)}=-\mu^{(c)}\frac{\Delta\psi}{\Delta u_z}, \tag{7}$$

with $\mu^{(c)}$ denoting the permeability of the crack interior, $D^{(c)}$ has been expressed in Eq. 1. In this paper, for convenience, the crack satisfying Eqs. 6, 7, and 1 is called *magnetically dielectric crack*.

It should be emphasized that when the crack is deformed under the applied magnetoelectromechanical loads, the thickness of the magnetically dielectric medium filling the crack will be changed. For a penny-shaped crack under axisymmetric loads, the opening crack profile should be an ellipsoid with a semi-major axis a and semi-minor axis b ($b \ll a$), which means in the cylinder coordinate system, the ellipsoidal surface can be expressed as

$$r^2/a^2+z^2/b^2=1. \tag{8}$$

As demonstrated by Zhang et al. (2006) for penny-shaped crack problems, both the normal electric displacement and magnetic induction inside the crack full of magnetically dielectric medium are uniform across the thickness of the deformed crack under uniformly magneoelectromechanical loads at infinity (see Eqs. 28 and 29 in Zhang et al. (2006)). And it has also been proved to be correct for dielectric penny-shaped crack problems (see e.g., Eq. 27 in Wang and Jiang (2004); Eq. 48 in Li and Lee (2004)). In addition, we remark that according to self-consistent method, the COD in Eqs. 7 and/or 1 can approximately be replaced with $2b\sqrt{1-r^2/a^2}$ (see McMeeking 1999 and Wang and Mai 2007 for piezoelectric crack problems, and Zhao et al. 2006 for magnetoelectroelastic crack problems).

It should also be noted that either the magnetically and/or electrically impermeable or permeable assumptions can be treated as two limiting cases of a magnetically dielectric crack. For example, letting $\varepsilon^{(c)}\to 0$ ($\mu^{(c)}\to 0$), $D^{(c)}=0$ ($B^{(c)}=0$) follows from Eq. 1 (Eq. 7), which is the premise of an electrically (magnetically) impermeable crack. On the other hand, if letting $\varepsilon^{(c)}\to\infty$ ($\mu^{(c)}\to\infty$), we get $\Delta\phi=0$ ($\Delta\psi=0$), it is identical to an electrically (magnetically) permeable crack. Moreover, the magnetoelectroelastic field corresponding to a magnetoelectrically permeable crack is assumed to be identical to that of a conducting crack with respect to both magnetic and electric fields. By the way, the above analysis is based on the consideration that a crack is permeable before deformation, and that both the magnetic and electric fields are exerted parallel to or perpendicular to the poling axis.

Because of the symmetry of the problem, it is sufficient to consider the upper-half plane of the penny-shaped crack. According to superposition theorem, the above-stated problem can be split up into two subproblems: one relating to a uniform field in a magnetoelectroelastic body without crack, and the other relating to a singular magnetoelectroelastic field due to the presence of a crack. From the viewpoint of fracture mechanics, it is sufficient to solve the corresponding problem posed by the following magnetoelectromechanical boundary conditions:

$$\sigma_{zz}(r,+\infty)=0,\quad \sigma_{zr}(r,+\infty)=0,$$
$$E_z(r,+\infty)=0,\quad H_z(r,+\infty)=0, \tag{9}$$

and

$$\sigma_{zz}(r,0)=-\sigma_0,\quad D_z(r,0)=D^{(c)}-D_0,$$
$$B_z(r,0)=B^{(c)}-B_0,\quad r<a, \tag{10a}$$

$$u_z(r,0)=0,\ \phi(r,0)=0,\ \psi(r,0)=0,\quad r\geq a, \tag{10b}$$

$$\sigma_{zr}(r,0)=0,\quad 0\leq r\leq+\infty, \tag{10c}$$

where

$$\sigma_0=\sigma_0, \tag{11a}$$

$$\begin{aligned}D_0=&\frac{1}{2c_{13}^2-(c_{11}+c_{12})c_{33}}\\&\times\Big[(2c_{13}e_{31}-c_{11}e_{33}-c_{12}e_{33})\sigma_0\\&+\Big(2c_{13}^2\varepsilon_{33}-2c_{33}e_{31}^2-c_{11}c_{33}\varepsilon_{33}-c_{12}c_{33}\varepsilon_{33}\\&-c_{11}e_{33}^2-c_{12}e_{33}^2+4c_{13}e_{31}e_{33}\Big)E_0\\&+\Big(2c_{13}^2g_{33}-2c_{33}e_{31}f_{31}-c_{11}c_{33}g_{33}\\&-c_{11}e_{33}f_{33}-c_{12}e_{33}f_{33}+2c_{13}e_{31}f_{33}\\&+2c_{13}e_{33}f_{31}\Big)H_0\Big],\end{aligned} \tag{11b}$$

$$\begin{aligned}B_0=&\frac{1}{2c_{13}^2-(c_{11}+c_{12})c_{33}}\\&\times\Big[\Big(2c_{13}f_{31}-c_{11}f_{33}-c_{12}f_{33}\Big)\sigma_0\\&+\Big(2c_{13}^2g_{33}-c_{11}c_{33}g_{33}-c_{12}c_{33}g_{33}\\&+2c_{13}e_{31}f_{33}-c_{11}e_{33}f_{33}-c_{12}e_{33}f_{33}\\&+2c_{13}e_{33}f_{31}-2c_{33}e_{31}f_{31}\Big)E_0\\&+\Big(2c_{13}^2\mu_{33}-c_{11}c_{33}\mu_{33}-c_{12}c_{33}\mu_{33}\\&+4c_{13}f_{31}f_{33}-c_{11}f_{33}^2-c_{12}f_{33}^2\\&-2c_{33}f_{31}^2\Big)H_0\Big]\end{aligned} \tag{11c}$$

For convenience, in what follows, σ_0, D_0, and B_0 are respectively called the mechanical, electrical, and magnetic loads equivalently applied on crack surfaces.

3 Method of solution

3.1 General solution of the governing equations

As usual, it is convenient to employ the Hankel transform technique to solve axisymmtric problems. In this study, we introduce a potential function by Hankel transform of the zeroth order

$$\begin{aligned}F(r,z)=&-\int_0^\infty\frac{1}{\xi}A(\xi)\exp(\gamma\xi z)\\&\times J_0(\xi r)\mathrm{d}\xi,\quad z\geq 0,\end{aligned} \tag{12}$$

and set

$$\begin{aligned}&u_r(r,z)=\frac{\partial F}{\partial r},\ u_z(r,z)=\eta_1\frac{\partial F}{\partial z},\ \phi(r,z)=\eta_2\frac{\partial F}{\partial z},\\&\psi(r,z)=\eta_3\frac{\partial F}{\partial z}.\end{aligned} \tag{13}$$

where A, γ, and $\eta_i(i=1,2,3)$ are, respectively, an unknown function and material constants to be determined, After substituting Eq. 13 together with 12 into Eq. 4, we obtain the general expressions for elastic displacements, electric potential and magnetic potential in terms of unknown function A_j as follows:

$$\begin{aligned}u_r(r,z)=&\sum_{j=1}^4\int_0^\infty A_j(\xi)\exp(\gamma_j\xi z)\\&\times J_1(\xi r)\mathrm{d}\xi,\end{aligned} \tag{14a}$$

$$\begin{aligned}u_z(r,z)=&-\sum_{j=1}^4\eta_{1j}\gamma_j\int_0^\infty A_j(\xi)\exp\left(\gamma_j\xi z\right)\\&\times J_0(\xi r)\mathrm{d}\xi,\end{aligned} \tag{14b}$$

$$\begin{aligned}\phi(r,z)=&-\sum_{j=1}^4\eta_{2j}\gamma_j\int_0^\infty A_j(\xi)\exp\left(\gamma_j\xi z\right)\\&\times J_0(\xi r)\mathrm{d}\xi,\end{aligned} \tag{14c}$$

$$\begin{aligned}\psi(r,z)=&-\sum_{j=1}^4\eta_{3j}\gamma_j\int_0^\infty A_j(\xi)\exp\left(\gamma_j\xi z\right)\\&\times J_0(\xi r)\mathrm{d}\xi,\end{aligned} \tag{14d}$$

where γ_j $(j=1,2,3,4)$ are chosen such that $Re\left(\gamma_j\right)$ are less than zero, which satisfy the following characteristic equation:

$$\det(\boldsymbol{\Xi})=0, \tag{15}$$

with

$$\boldsymbol{\Xi}=\begin{bmatrix}c_{11}-c_{44}\gamma_j^2 & (c_{11}+c_{44})\gamma_j & (e_{31}+e_{15})\gamma_j & (f_{31}+f_{15})\gamma_j\\(c_{11}+c_{44})\gamma_j & c_{33}\gamma_j^2-c_{44} & e_{33}\gamma_j^2-e_{15} & f_{33}\gamma_j^2-f_{15}\\(e_{31}+e_{15})\gamma_j & e_{33}\gamma_j^2-e_{15} & \varepsilon_{11}-\varepsilon_{33}\gamma_j^2 & g_{11}-g_{33}\gamma_j^2\\(f_{31}+f_{15})\gamma_j & f_{33}\gamma_j^2-f_{15} & g_{11}-g_{33}\gamma_j^2 & \mu_{11}-\mu_{33}\gamma_j^2\end{bmatrix}, \tag{16}$$

and η_{1j}, η_{2j}, and η_{3j} satisfy the following equations:

$$\boldsymbol{\Xi}\left\{1\quad -\eta_{1j}\gamma_j\quad -\eta_{2j}\gamma_j\quad -\eta_{3j}\gamma_j\right\}^{\mathrm{T}}=\mathbf{0}. \tag{17}$$

From the constitutive equations, the expressions for stresses, electric displacement, and magnetic induction

for $z \geq 0$ can easily be obtained in terms of A_j as follows

$$\sigma_{zz}(r,z) = \sum_{j=1}^{4} \beta_{1j} \int_0^\infty \xi A_j(\xi) \exp\left(\gamma_j \xi z\right) \times J_0(\xi r) \mathrm{d}\xi, \tag{18a}$$

$$\sigma_{rz}(r,z) = \sum_{j=1}^{4} \beta_{2j} \int_0^\infty \xi A_j(\xi) \exp\left(\gamma_j \xi z\right) \times J_1(\xi r) \mathrm{d}\xi, \tag{18b}$$

$$D_z(r,z) = \sum_{j=1}^{4} \beta_{3j} \int_0^\infty \xi A_j(\xi) \exp\left(\gamma_j \xi z\right) \times J_0(\xi r) \mathrm{d}\xi, \tag{18c}$$

$$B_z(r,z) = \sum_{j=1}^{4} \beta_{4j} \int_0^\infty \xi A_j(\xi) \exp\left(\gamma_j \xi z\right) \times J_0(\xi r) \mathrm{d}\xi, \tag{18d}$$

where

$$\beta_{1j} = c_{13} - \left(c_{33}\eta_{1j} + e_{33}\eta_{2j} + f_{33}\eta_{3j}\right)\gamma_j^2, \tag{19a}$$

$$\beta_{2j} = \left[c_{44}\left(1+\eta_{1j}\right) + e_{15}\eta_{2j} + f_{15}\eta_{3j}\right]\gamma_j, \tag{19b}$$

$$\beta_{3j} = e_{31} - \left(e_{33}\eta_{1j} - \varepsilon_{33}\eta_{2j} - g_{33}\eta_{3j}\right)\gamma_j^2, \tag{19c}$$

$$\beta_{4j} = f_{31} - \left(f_{33}\eta_{1j} - g_{33}\eta_{2j} - \mu_{33}\eta_{3j}\right)\gamma_j^2. \tag{19d}$$

3.2 Derivation of algebra equations and solution

For convenience, we denote the components of elastic displacement, electric potential, and magnetic potential in the crack plane as $u_z(r) = u_z(r,0)$, $\phi(r) = \phi(r,0)$, and $\psi(r) = \psi(r,0)$, respectively. Similarly, the components of stress, electric displacement, and magnetic induction in the crack plane are denoted as $\sigma_{zz}(r)$, $D_z(r)$, $B_z(r)$, respectively. Thus, we can obtain from Eq. 14

$$u_z(r) = -\sum_{j=1}^{4} \eta_{1j}\gamma_j \int_0^\infty A_j(\xi) J_0(\xi r) \mathrm{d}\xi, \tag{20a}$$

$$\phi(r) = -\sum_{j=1}^{4} \eta_{2j}\gamma_j \int_0^\infty A_j(\xi) J_0(\xi r) \mathrm{d}\xi, \tag{20b}$$

$$\psi(r) = -\sum_{j=1}^{4} \eta_{3j}\gamma_j \int_0^\infty A_j(\xi) J_0(\xi r) \mathrm{d}\xi. \tag{20c}$$

We now introduce three unknown auxiliary functions $U(r)$, $\Phi(r)$, and $\Psi(r)$, which satisfy the following equations:

$$\sum_{j=1}^{4} \eta_{1j}\gamma_j A_j(\xi) = -\int_0^a U(t)\sin(\xi t)\,\mathrm{d}t, \tag{21a}$$

$$\sum_{j=1}^{4} \eta_{2j}\gamma_j A_j(\xi) = -\int_0^a \Phi(t)\sin(\xi t)\,\mathrm{d}t, \tag{21b}$$

$$\sum_{j=1}^{4} \eta_{3j}\gamma_j A_j(\xi) = -\int_0^a \Psi(t)\sin(\xi t)\,\mathrm{d}t. \tag{21c}$$

Substituting Eq. 21 into Eq. 20 and recalling the known result

$$\int_0^\infty J_0(\xi r)\sin(\xi t)\,\mathrm{d}\xi = \frac{H(t-r)}{\sqrt{t^2-r^2}}, \tag{22}$$

where $H(\bullet)$ is the Heaviside step function, we find that the boundary conditions in Eq. 10b are automatically satisfied. Moreover, the displacement, electric potential, and magnetic potential at the crack face can be expressed as

$$u_z(r) = \int_r^a \frac{U(t)}{\sqrt{t^2-r^2}}\mathrm{d}t,\ \phi(r) = \int_r^a \frac{\Phi(t)}{\sqrt{t^2-r^2}}\mathrm{d}t,$$
$$\psi(r) = \int_r^a \frac{\Psi(t)}{\sqrt{t^2-r^2}}\mathrm{d}t,\quad r < a. \tag{23}$$

Equation 21 in connection with the application of Eqs. 10c and 18b forms a system of linear algebraic equations for A_j $(j = 1, 2, 3, 4)$, from which we get

$$A_j(\xi) = -\alpha_{1j}\int_0^a U(t)\sin(\xi t)\mathrm{d}t - \alpha_{2j}\int_0^a \Phi(t)\sin(\xi t)\mathrm{d}t - \alpha_{3j}\int_0^a \Psi(t)\sin(\xi t)\mathrm{d}t, \tag{24}$$

where

$$\alpha_{ij} = \bar{Q}_{ij}/\det(\mathbf{Q}), \quad i = 1, 2, 3, \ \ j = 1, 2, 3, 4, \quad (25)$$

and $\mathbf{Q}$ is a 4×4 matrix, the elements of which are

$$\begin{aligned} Q_{ij} &= \eta_{ij}\gamma_j, \quad i = 1, 2, 3, \\ \Omega_{4j} &= \beta_{2j}, \quad j = 1, 2, 3, 4, \end{aligned} \quad (26)$$

and $\bar{Q}_{ij}$ are the corresponding algebraic cofactors of Q_{ij}.

Substituting Eq. 24 into Eqs. 18a, 18c, and 18d for the crack plane $z = 0$, and making use of the boundary conditions in Eq. 10a yield

$$\sum_{j=1}^{4} \beta_{1j} \int_0^a \left[\alpha_{1j} U(t) + \alpha_{2j}\Phi(t) + \alpha_{3j}\Psi(t)\right] \times \int_0^\infty \xi \sin(\xi t) J_0(\xi r) \mathrm{d}\xi \mathrm{d}t = \sigma_0, \quad r < a, \quad (27a)$$

$$\sum_{j=1}^{4} \beta_{3j} \int_0^a \left[\alpha_{1j} U(t) + \alpha_{2j}\Phi(t) + \alpha_{3j}\Psi(t)\right] \times \int_0^\infty \xi \sin(\xi t) J_0(\xi r) \mathrm{d}\xi \mathrm{d}t = D_0 - D^{(c)}, \quad r < a, \quad (27b)$$

$$\sum_{j=1}^{4} \beta_{4j} \int_0^a \left[\alpha_{1j} U(t) + \alpha_{2j}\Phi(t) + \alpha_{3j}\Psi(t)\right] \times \int_0^\infty \xi \sin(\xi t) J_0(\xi r) \mathrm{d}\xi \mathrm{d}t = B_0 - B^{(c)}, \quad r < a. \quad (27c)$$

Multiplying $r/\left(x^2 - r^2\right)^{1/2}$ to two sides of Eqs. 27a, 27b, and 27c, and then integrating with respect to r from 0 to $x \quad (x < a)$, respectively, we finally obtain

$$m_{11}U(x) + m_{12}\Phi(x) + m_{13}\Psi(x) = \frac{2}{\pi}\sigma_0 x, \quad x < a, \quad (28a)$$

$$m_{21}U(x) + m_{22}\Phi(x) + m_{23}\Psi(x) = \frac{2}{\pi}\left(D_0 - D^{(c)}\right)x, \quad x < a, \quad (28b)$$

$$m_{31}U(x) + m_{32}\Phi(x) + m_{33}\Psi(x) = \frac{2}{\pi}\left(B_0 - B^{(c)}\right)x, \quad x < a, \quad (28c)$$

where

$$\begin{aligned} m_{1l} &= \sum_{j=1}^{4} \beta_{1j}\alpha_{lj}, \quad l = 1, 2, 3, \\ m_{kl} &= \sum_{j=1}^{4} \beta_{(k+1)j}\alpha_{lj}, \quad k = 2, 3, \ \ l = 1, 2, 3. \end{aligned} \quad (29)$$

In the procedure of deriving Eq. 28, the following relations

$$\int_0^x \frac{r J_0(\xi r)}{\sqrt{x^2 - r^2}} \mathrm{d}r = \frac{\sin(\xi x)}{\xi}, \quad (30)$$

$$\int_0^\infty \sin(\xi t) \sin(\xi x) \, \mathrm{d}\xi = \frac{\pi}{2}\delta(x - t), \quad (31)$$

with $\delta(\bullet)$ being the Dirac delta function, have been applied.

By directly solving Eq. 28, we have

$$U = \frac{2x}{\pi} \frac{\bar{m}_{11}\sigma_0 + \bar{m}_{21}\left(D_0 - D^{(c)}\right) + \bar{m}_{31}\left(B_0 - B^{(c)}\right)}{\det(\mathbf{m})}, \quad (32a)$$

$$\Phi = \frac{2x}{\pi} \frac{\bar{m}_{12}\sigma_0 + \bar{m}_{22}\left(D_0 - D^{(c)}\right) + \bar{m}_{32}\left(B_0 - B^{(c)}\right)}{\det(\mathbf{m})}, \quad (32b)$$

$$\Psi = \frac{2x}{\pi} \frac{\bar{m}_{13}\sigma_0 + \bar{m}_{23}\left(D_0 - D^{(c)}\right) + \bar{m}_{33}\left(B_0 - B^{(c)}\right)}{\det(\mathbf{m})}, \quad (32c)$$

where $\mathbf{m} = \left[m_{ij}\right]$, and $\bar{m}_{ij}$, as pointed out before, are the algebraic cofactors of m_{ij}.

From Eqs. 1, 7, and 23, it is easily found that $D^{(c)}$ and $B^{(c)}$ can be evaluated by the following nonlinear algebraic equations:

$$D^{(c)} = -\varepsilon^{(c)} \frac{\bar{m}_{12}\sigma_0 + \bar{m}_{22}\left(D_0 - D^{(c)}\right) + \bar{m}_{32}\left(B_0 - B^{(c)}\right)}{\bar{m}_{11}\sigma_0 + \bar{m}_{21}\left(D_0 - D^{(c)}\right) + \bar{m}_{31}\left(B_0 - B^{(c)}\right)}, \quad (33a)$$

$$B^{(c)} = -\mu^{(c)} \frac{\bar{m}_{13}\sigma_0 + \bar{m}_{23}\left(D_0 - D^{(c)}\right) + \bar{m}_{33}\left(B_0 - B^{(c)}\right)}{\bar{m}_{11}\sigma_0 + \bar{m}_{21}\left(D_0 - D^{(c)}\right) + \bar{m}_{31}\left(B_0 - B^{(c)}\right)}. \quad (33b)$$

By carrying out a simple manipulation, a linear triple-equation with unknown $D^{(c)}$ or $B^{(c)}$ can be obtained. Thus, $D^{(c)}$ and $B^{(c)}$ can easily be solved (see Appendix A). As shown in Appendix A, for a general magnetically dielectric crack full of $\mu^{(c)}$ and $\varepsilon^{(c)}$, there exists three roots for both $D^{(c)}$ and $B^{(c)}$. Therefore, there are two superfluous roots for either $D^{(c)}$ or $B^{(c)}$. From the physical argument, a reasonable $D^{(c)}$ and/or $B^{(c)}$ should be selected to avoid overlapping of crack surfaces, i.e., satisfying the crack opening condition $u_z(x) \geq 0$.

3.3 Electric displacement and magnetic induction inside the crack under special crack surface assumptions

From Eq. 33, it is easily seen that apart from the material properties of the magnetoelectroelastic body, either $D^{(c)}$ or $B^{(c)}$ is also dependent on electric permittivity $\varepsilon^{(c)}$ and magnetic permeability $\mu^{(c)}$ of the interior of the opening crack, and dependent on mechanical, electrical, and magnetic loads equivalently applied on the crack surfaces, i.e., σ_0, D_0, and B_0.

Particularly, for four special crack surface boundary conditions, i.e., (i) magnetically impermeable and electrically impermeable, (ii) magnetically impermeable and electrically permeable, (iii) magnetically permeable and electrically impermeable and (iv) magnetically permeable and electrically permeable, simple expressions for $D^{(c)}$ and $B^{(c)}$ may directly be derived from Eq. 33 as well. They are, respectively,

(i) for a magnetoelectrically impermeable crack $\left(\varepsilon^{(c)} = 0,\ \mu^{(c)} = 0\right)$,

$$D^{(c)} = 0,\ B^{(c)} = 0; \tag{34}$$

(ii) for a magnetically impermeable and electrically permeable crack $\left(\varepsilon^{(c)} = \infty,\ \mu^{(c)} = 0\right)$,

$$D^{(c)} = \frac{m_{21}m_{33} - m_{23}m_{31}}{m_{13}m_{31} - m_{11}m_{33}}\sigma_0 + D_0 + \frac{m_{11}m_{23} - m_{13}m_{21}}{m_{13}m_{31} - m_{11}m_{33}}B_0,\quad B^{(c)} = 0; \tag{35}$$

(iii) for a magnetically permeable and electrically impermeable crack $\left(\varepsilon^{(c)} = 0,\ \mu^{(c)} = \infty\right)$,

$$D^{(c)} = 0,\ B^{(c)} = \frac{m_{22}m_{31} - m_{21}m_{32}}{m_{12}m_{21} - m_{11}m_{22}}\sigma_0 + \frac{m_{11}m_{32} - m_{12}m_{31}}{m_{12}m_{21} - m_{11}m_{22}}D_0 + B_0; \tag{36}$$

(iv) for a magnetoelectrically conducting crack $\left(\varepsilon^{(c)} = \infty,\ \mu^{(c)} = \infty\right)$

$$D^{(c)} = D_0 - \frac{m_{21}}{m_{11}}\sigma_0,\ B^{(c)} = B_0 - \frac{m_{31}}{m_{11}}\sigma_0. \tag{37}$$

4 Analysis on the field quantities and field intensity factors

Once $B^{(c)}$ and $D^{(c)}$ are sought, the solution of $U(x)$, $\Phi(x)$ and $\Psi(x)$ are readily obtained by Eq. 32. Evaluating the integrals in Eq. 23, the COD, electric potential difference and magnetic potential difference at the crack surface can be obtained as follows

$$u_z(r) = \frac{2}{\pi}\frac{\bar{m}_{11}\sigma_0 + \bar{m}_{21}\left(D_0 - D^{(c)}\right) + \bar{m}_{31}\left(B_0 - B^{(c)}\right)}{\det(\mathbf{m})} \times\sqrt{a^2 - r^2}, \tag{38a}$$

$$\phi(r) = \frac{2}{\pi}\frac{\bar{m}_{12}\sigma_0 + \bar{m}_{22}\left(D_0 - D^{(c)}\right) + \bar{m}_{32}\left(B_0 - B^{(c)}\right)}{\det(\mathbf{m})} \times\sqrt{a^2 - r^2}, \tag{38b}$$

$$\psi(r) = \frac{2}{\pi}\frac{\bar{m}_{13}\sigma_0 + \bar{m}_{23}\left(D_0 - D^{(c)}\right) + \bar{m}_{33}\left(B_0 - B^{(c)}\right)}{\det(\mathbf{m})} \times\sqrt{a^2 - r^2}. \tag{38c}$$

Substituting Eq. 32 into Eq. 24 and then into Eqs. 18a, 18c, and 18d for the crack plane $z = 0$, it is found that

$$\sigma_{zz}(r) = -\frac{2\sigma_0}{\pi}\int_0^a t\int_0^\infty \xi\,\sin(\xi t)J_0(\xi r)\mathrm{d}\xi\,\mathrm{d}t, \tag{39a}$$

$$D_z(r) = -\frac{2\left[D_0 - D^{(c)}\right]}{\pi}\int_0^a t\int_0^\infty \xi\,\sin(\xi t) \times J_0(\xi r)\mathrm{d}\xi\,\mathrm{d}t, \tag{39b}$$

$$B_z(r) = -\frac{2\left[B_0 - B^{(c)}\right]}{\pi}\int_0^a t\int_0^\infty \xi\,\sin(\xi t) \times J_0(\xi r)\mathrm{d}\xi\,\mathrm{d}t. \tag{39c}$$

Noting

$$\frac{\mathrm{d}}{\mathrm{d}r}\left[rJ_1(\xi r)\right] = \xi r J_0(\xi r),\quad \int_0^\infty \sin(\xi t)J_1(\xi r)\mathrm{d}\xi = \frac{tH\,(r-t)}{r\sqrt{r^2 - t^2}}, \tag{40}$$

the integral in Eq. 39 can be given as

$$\int_0^a t \int_0^\infty \xi \sin(\xi t) J_0(\xi r) \mathrm{d}\xi \mathrm{d}t = \frac{1}{r}\frac{\mathrm{d}}{\mathrm{d}r}\int_0^a \frac{t^2 H(r-t)}{\sqrt{r^2-t^2}}\mathrm{d}t = \begin{cases} \pi/2, & r < a, \\ \sin^{-1}(a/r) - a/\sqrt{r^2-a^2}, & r > a. \end{cases} \tag{41}$$

Obviously, the above result for $r < a$ fulfills the boundary conditions at the crack surfaces, and the result for $r > a$ is useful in determining the magnetoelectroelastic behaviors ahead of crack front.

We define

$$K^q = \lim_{r \to a^+} \sqrt{2\pi (r-a)} q(r), \tag{42}$$

where $q(r) \equiv q(r, 0)$ stands for σ_{zz}, D_z, and B_z, respectively. Then the intensity factors of stress, electric displacement, and magnetic induction can be expressed as

$$K^\sigma = \frac{2}{\pi}\sqrt{\pi a}\sigma_0, \quad K^D = \frac{2}{\pi}\sqrt{\pi a}\left[D_0 - D^{(c)}\right], \quad K^B = \frac{2}{\pi}\sqrt{\pi a}\left[B_0 - B^{(c)}\right]. \tag{43}$$

Equation 43 implies that no matter how magnetic and/or electric loads applied on the crack surfaces vary, stress intensity factors remain unchanged if σ_0 is a prescribed constant, while both electric displacement and magnetic induction intensity factors depend on not only the mechanical load but also the electrical and magnetic loads. Moreover, both the electric displacement and magnetic induction intensity factors depend on the material properties and $\varepsilon^{(c)}$ and $\mu^{(c)}$ as well.

Additionally, for the COD across the crack near the crack front, according to the following definition

$$K_{\mathrm{COD}} = \lim_{r \to a^-} \sqrt{\frac{\pi}{2(a-r)}} u_z(r), \tag{44}$$

we can obtain the COD intensity factor as

$$K_{\mathrm{COD}} = \frac{2}{\pi}\sqrt{\pi a}\frac{\bar{m}_{11}\sigma_0 + \bar{m}_{21}\left(D_0 - D^{(c)}\right) + \bar{m}_{31}\left(B_0 - B^{(c)}\right)}{\det(\mathbf{m})}. \tag{45}$$

This indicates that, similar to K^D and/or K^B, the COD intensity factor K_{COD} depends on material properties, loading cases together with magnetic permeability and dielectric permittivity inside the crack.

In addition, for a magnetically impermeable crack, $B^{(c)} = 0$ at the crack surfaces. Therefore, the magnetic induction intensity factors in this case directly depend only on the magnetic load B_0, not on the mechanical load σ_0 and electric load D_0, which is in agreement with those for a crack in an infinite magnetoelectroelastic strip under the impermeable assumption for antiplane analysis (Hu and Li 2005). And for an electrically impermeable crack, there exists similar phenomena, which have also been observed for a crack in an infinite piezoelectric ceramics in two-dimensional and three-dimensional analyses (Pak 1992; Jiang and Sun 2001). On the other hand, if only adopting magnetoelectrically permeable boundary conditions, as pointed out before, the corresponding solution is equal to that of a conducting crack in the present analysis. The application of Eq. 37 to the above field intensity factors results in

$$K^\sigma = \frac{2}{\pi}\sqrt{\pi a}\sigma_0, \quad K^D = \frac{2m_{21}}{\pi m_{11}}\sqrt{\pi a}\sigma_0, \quad K^B = \frac{2m_{31}}{\pi m_{11}}\sqrt{\pi a}\sigma_0, \tag{46a}$$

$$K_{\mathrm{COD}} = \frac{2}{\pi m_{11}}\sqrt{\pi a}\sigma_0, \tag{46b}$$

which indicates that for a magnetoelectrically permeable crack, the stress, electric displacement, magnetic induction and COD all exhibit a square-root singularity near the crack front. Furthermore the singularity arises only from the mechanical load σ_0, not from the magnetic load B_0 and/or electric load D_0, which further implies that the singularity is independent of both the magnetic and electric fields applied at infinity. These phenomena are in consistence with those in Gao et al. (2003) and Zhou et al. (2004) for antiplane megneto-electroelastic analysis and those in Kogan et al. (1996) and Yang and Li (2002) for three-dimensional piezoelectric ceramics analysis.

5 Numerical results and discussions

According to the classical COD fracture criterion for a three-dimensional elastic body, crack starts to grow when the COD intensity factor exceeds the critical value under the applied loads. For a magnetoelectroelastic material, not only mechanical loads but also magnetic and electrical loads can cause a crack to open and even to propagate. In this section, a numerical example is

given to examine the effects of the applied magnetic and/or electric fields on the COD intensity factor near the crack front.

Numerical calculations are carried out for a penny-shaped crack in a $BaTiO_3$–$CoFe_2O_4$ composite, the material properties of which are taken from Wang and Mai (2007). Without loss of generality, in all our calculating procedures, it is assumed that $\sigma_0 = 4.2 \times 10^6\,\mathrm{N/m^2}$. Numerical results are plotted in Figs. 2–4, where K_0 represents the COD intensity factor of magnetoelectrically impermeable penny-shaped crack in an infinite magnetoelectroelastic solid under only mechanical load; $\lambda_H = f_{33}H_0/\sigma_0$ and $\lambda_E = e_{33}E_0/\sigma_0$ are two parameters introduced to reflect the corresponding loading combinations between magnetic and mechanical loads, and between electrical and mechanical loads, respectively; ε_r and μ_r are defined as

$$\varepsilon_r = \varepsilon_c/\varepsilon_0,\ \ \mu_r = \mu_c/\mu_0, \tag{47}$$

with $\varepsilon_0 = 0.0885\times10^{-10}\,\mathrm{C^2/Nm^2}$ and $\mu_0 = 0.1256\times 10^{-5}\,\mathrm{Ns^2/C^2}$ being the electric permittivity and magnetic permeability of air (or vacuum), respectively. Obviously, in general, $\varepsilon_r = 1$ and $\mu_r = 1$, which means the crack is magnetically dielectric, while $\varepsilon_r = 0$ (or $\mu_r = 0$) and $\varepsilon_r = \infty$ (or $\mu_r = \infty$) imply that the crack is electrically (or magnetically) impermeable and electrically (or magnetically) permeable, respectively.

Figures 2 and 3 indicate that for a crack full of air or vacuum (i.e., magnetically dielectric crack), according to the maximum COD criterion, negative magnetic fields slightly inhibit crack propagation and growth, while positive magnetic fields slightly enhance crack propagation. Figure 4 indicates that electric fields have the same effects on K_{COD} as applied magnetic fields have.

From these figures, it is seen that adopting magnetically (or electrically) impermeable assumptions, magnetic (or electric) fields have great effects on K_{COD}, i.e., magnetic (or electric) fields can evidently aid or impede crack growth, not only depending on the sizes but also the directions of applied magnetic (or electric) fields. The effects of the electric fields on K_{COD} for the magnetoelectroelastic body are in agreement with the corresponding results for piezoelectric ceramic (Park and Sun 1995; Li and Lee 2004). Moreover, in the case of $\mu_r = 0$ (or $\varepsilon_r = 0$), for a given λ_E (or λ_H), there is a critical value of λ_H (or λ_E) in the range of our calculations, when λ_H (or λ_E) is less than the corresponding

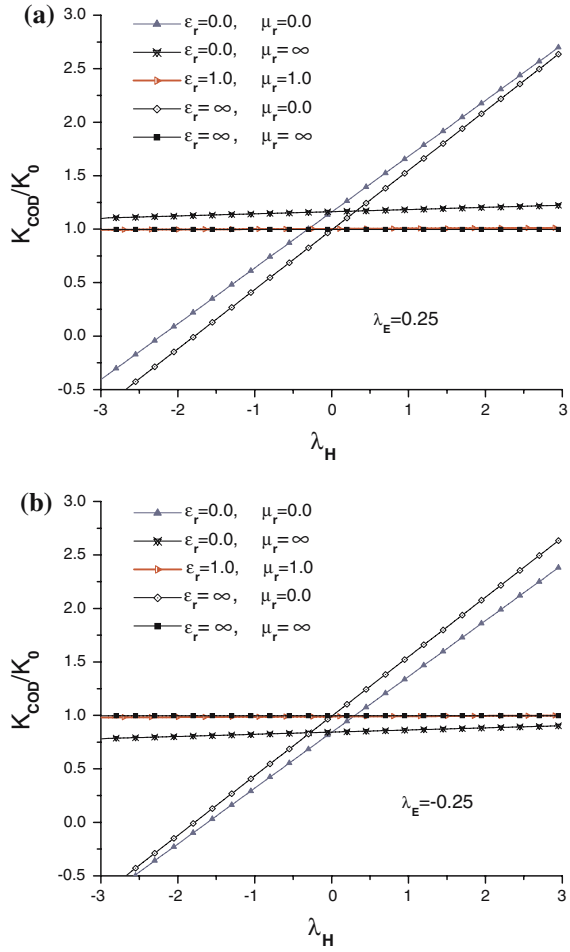

Fig. 2 Normalized COD intensity factors as a function of combined magnetic and mechanical loading $\lambda_H = \mathrm{f}_{33}H_0/\sigma_0$ for different crack surface conditions under combined electric and mechanical loadings $\lambda_E = \mathrm{e}_{33}E_0/\sigma_0$: (**a**) $\lambda_E = 0.25$; (**b**) $\lambda_E = -0.25$

critical value, the calculated K_{COD} is less than zero. It perhaps should be explained that the crack is actually closed at this moment. We remark that for a magnetically dielectric crack, both the critical magnetic and electrical fields have not been found in the depicted figures.

As expected, in the case of magnetically (or electrically) permeable crack assumptions, for given electric (or magnetic) fields, the effects of magnetic (or electric) fields on crack propagation and growth are much less than those for the corresponding magnetically (or electrically) impermeable crack surface assumptions. Especially, for both magnetically and electrically permeable assumptions, K_{COD} is independent of either

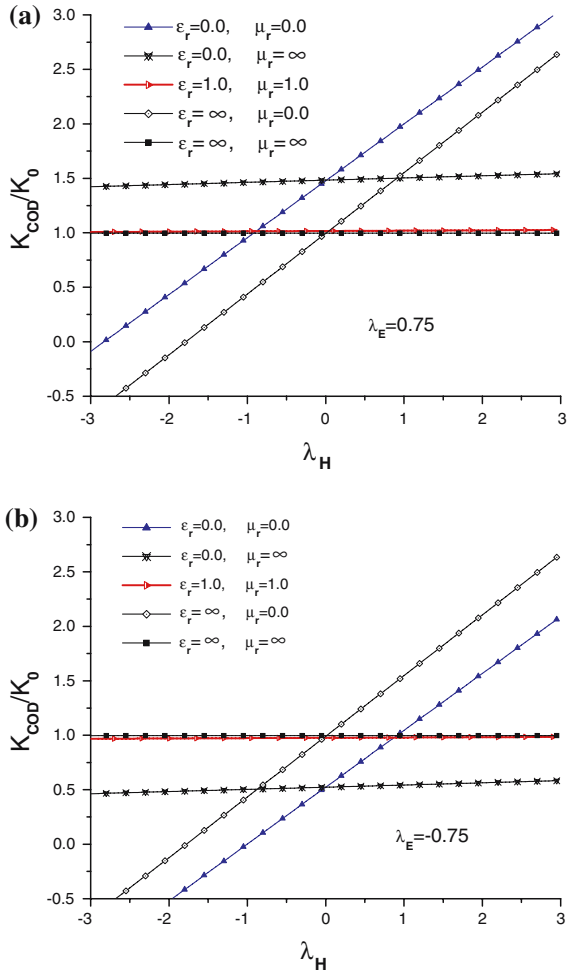

Fig. 3 Normalized COD intensity factors as a function of combined magnetic and mechanical loading $\lambda_H = \mathrm{f}_{33}H_0/\sigma_0$ for different crack surface conditions under combined electric and mechanical loadings $\lambda_E = \mathrm{e}_{33}E_0/\sigma_0$: (**a**) $\lambda_E = 0.75$; (**b**) $\lambda_E = -0.75$

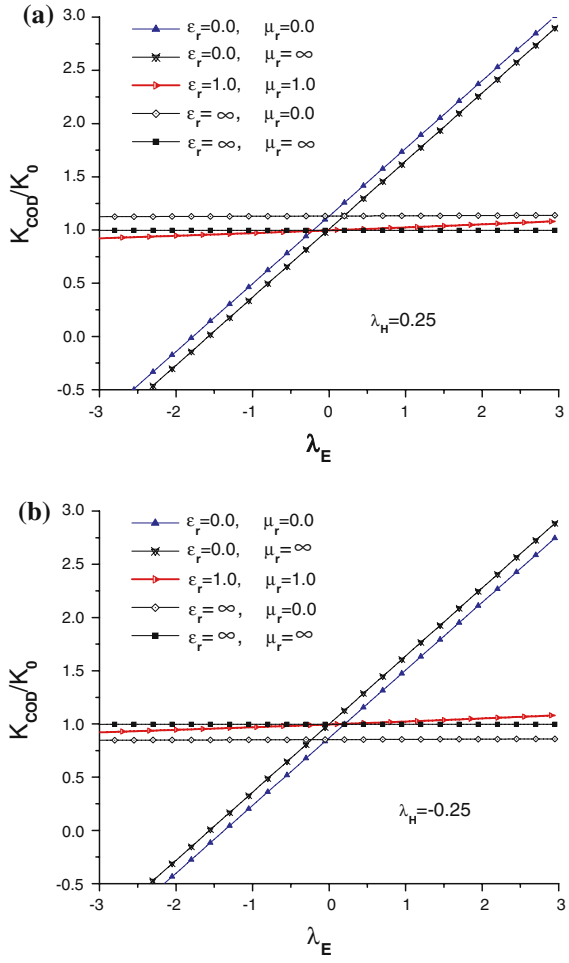

Fig. 4 Normalized COD intensity factors as a function of combined electric and mechanical loading $\lambda_E = \mathrm{e}_{33}E_0/\sigma_0$ for different crack surface conditions under combined magnetic and mechanical loadings $\lambda_H = \mathrm{f}_{33}H_0/\sigma_0$: (**a**) $\lambda_H = 0.25$; (**b**) $\lambda_H = -0.25$

applied magnetic field H_0 or electric field E_0. This is in agreement with the reduced result, i.e., Eq. 46b, which could imply that our calculated results are correct.

Finally, it should be noted that for a penny-shaped crack full of magnetically dielectric medium, the four kinds of ideal models of analyzing the response to magnetic and/or electric fields, to some extent, can all cause some errors. Comparatively speaking, as shown in Figs. 2–4, similar to piezoelectric crack problems pointed out in Sect. 1, for the material properties used here, magnetically and/or electrically impermeable assumptions would introduce large errors on K_{COD} than permeable assumptions.

6 Conclusions

The magnetoelectroelastic analysis of a transversely isotropic magnetoelectroelastic body with a magnetically dielectric penny-shaped crack perpendicular to the poling direction was conducted. The problem was solved under the exact magnetoelectric boundary condition, i.e., the crack is magnetically dielectric. By making use of the Hankel transform technique, the mixed boundary value problem was converted to the algebraic equations with respect to three auxiliary functions. Both the magnetic induction $B^{(c)}$ and electric displacement $D^{(c)}$ induced by the crack are obtained

explicitly. The field intensity factors were also derived in a closed form and discussed in detail. For a magnetically dielectric crack, except for the stress intensity factor, all the other intensity factors are apparently affected by the magnetic permeability and dielectric permittivity of the crack interior, magnetoelectromechanical loads equivalently applied on the crack surfaces and material properties. Previous studies on magnetoelectrically impermeable or permeable penny-shaped cracks can be reduced from the present analysis as limiting cases.

According to the maximum COD criterion, for magnetically dielectric cracks, both negative magnetic and electrical fields impede crack propagation and growth, and both positive magnetic and electric fields enhance crack propagation. However, the effects of both magnetic and electrical loads on the crack propagation and growth under the exact crack surface conditions are much less than the corresponding ones under the magnetoelectrically impermeable crack surface assumption.

Acknowledgements The work was supported by the small project funding of University Research Grants (URG) (2006–2007), The University of Hong Kong, and the Natural Science Funding of Hebei Province, China.

Appendix A

$$D_1^{(c)} = -\frac{a_2}{3a_3} - \frac{\sqrt[3]{2}}{3a_3}\frac{\chi_2}{\chi_1} + \frac{\chi_1}{3\sqrt[3]{2}a_3}, \tag{A.1}$$

$$D_2^{(c)} = -\frac{a_2}{3a_3} + \frac{\left(1+i\sqrt{3}\right)\chi_2}{3\sqrt[3]{4}a_3\chi_1} - \frac{\left(1-i\sqrt{3}\right)\chi_1}{6\sqrt[3]{2}a_3}, \tag{A.2}$$

$$D_3^{(c)} = -\frac{a_2}{3a_3} + \frac{\left(1-i\sqrt{3}\right)\chi_2}{3\sqrt[3]{4}a_3\chi_1} - \frac{\left(1+i\sqrt{3}\right)\chi_1}{6\sqrt[3]{2}a_3}, \tag{A.3}$$

$$B_i^{(c)} = \frac{\bar{m}_{31}B_0D_i^{(c)} + \bar{m}_{21}D_0D_i^{(c)} - \bar{m}_{21}D_i^{(c)2} - \bar{m}_{22}D_i^{(c)}\varepsilon^{(c)} + \bar{m}_{11}D_i^{(c)}\sigma_0}{\bar{m}_{31}D_i^{(c)} + \bar{m}_{32}\varepsilon^{(c)}} + \frac{\bar{m}_{32}B_0\varepsilon^{(c)} + \bar{m}_{22}D_0\varepsilon^{(c)} + \bar{m}_{12}\varepsilon^{(c)}\sigma_0}{\bar{m}_{31}D_i^{(c)} + \bar{m}_{32}\varepsilon^{(c)}}, \quad i = 1, 2, 3, \tag{A.4}$$

where

$$\chi_1 = \left(-2a_2^3 + 9a_1a_2a_3 - 27a_0a_3^2 + \sqrt{4\left(3a_1a_3 - a_2^2\right)^3 + \left(-2a_2^3 + 9a_1a_2a_3 - 27a_0a_3^2\right)^2}\right)^{1/3}, \tag{A.5}$$

$$\chi_2 = 3a_1a_3 - 2a_2^2, \tag{A.6}$$

$$\begin{aligned} a_0 = {} & \varepsilon^{(c)2}\left(-\bar{m}_{22}^2\bar{m}_{31}D_0^2 + \bar{m}_{23}\bar{m}_{32}^2D_0\mu^{(c)} - \bar{m}_{12}\bar{m}_{31}\bar{m}_{32}B_0\sigma_0\right. \\ & + \bar{m}_{11}\bar{m}_{32}^2B_0\sigma_0 + \bar{m}_{13}\bar{m}_{32}^2\mu^{(c)}\sigma_0 - \bar{m}_{12}\bar{m}_{32}\bar{m}_{33}\mu^{(c)}\sigma_0 \\ & - \bar{m}_{12}^2\bar{m}_{31}\sigma_0^2 + \bar{m}_{11}\bar{m}_{12}\bar{m}_{32}\sigma_0^2 \\ & + \bar{m}_{21}\bar{m}_{32}D_0\left(\bar{m}_{32}B_0 + \bar{m}_{12}\sigma_0\right) \\ & + \bar{m}_{22}D_0\left(\bar{m}_{32}\left(\bar{m}_{21}D_0 - \bar{m}_{33}\mu^{(c)} + \bar{m}_{11}\sigma_0\right)\right. \\ & \left.\left. - \bar{m}_{31}\left(\bar{m}_{32}B_0 + 2\bar{m}_{12}\sigma_0\right)\right)\right), \end{aligned} \tag{A.7}$$

$$\begin{aligned} a_1 = {} & \varepsilon^{(c)}\left(\bar{m}_{21}^2\bar{m}_{32}D_0^2 + 2\bar{m}_{22}^2\bar{m}_{31}D_0\varepsilon^{(c)}\right. \\ & + 2\bar{m}_{23}\bar{m}_{31}\bar{m}_{32}D_0\mu^{(c)} \\ & - \bar{m}_{23}\bar{m}_{32}^2\varepsilon^{(c)}\mu^{(c)} - \bar{m}_{12}\bar{m}_{31}^2B_0\sigma_0 + \bar{m}_{11}\bar{m}_{31}\bar{m}_{32}B_0\sigma_0 \\ & + 2\bar{m}_{13}\bar{m}_{31}\bar{m}_{32}\mu^{(c)}\sigma_0 - \bar{m}_{12}\bar{m}_{31}\bar{m}_{33}\mu^{(c)}\sigma_0 \\ & - \bar{m}_{11}\bar{m}_{32}\bar{m}_{33}\mu^{(c)}\sigma_0 - \bar{m}_{11}\bar{m}_{12}\bar{m}_{31}\sigma_0^2 + \bar{m}_{11}^2\bar{m}_{32}\sigma_0^2 - \bar{m}_{22} \\ & \times\left(\bar{m}_{31}^2B_0D_0 + \bar{m}_{32}\varepsilon^{(c)}\left(2\bar{m}_{21}D_0 - \bar{m}_{33}\mu^{(c)} + \bar{m}_{11}\sigma_0\right)\right. \\ & + \bar{m}_{31}\left(\bar{m}_{21}D_0^2 - \bar{m}_{32}B_0\varepsilon^{(c)} + \bar{m}_{33}D_0\mu^{(c)} + \bar{m}_{11}D_0\sigma_0\right. \\ & \left.\left.\left. - 2\bar{m}_{12}\ \varepsilon^{(c)}\sigma_0\right)\right) + \bar{m}_{21}\left(\bar{m}_{31}D_0\left(\bar{m}_{32}B_0 - \bar{m}_{12}\sigma_0\right)\right. \\ & - \bar{m}_{32}\left(\bar{m}_{32}B_0\varepsilon^{(c)} + \bar{m}_{33}D_0\mu^{(c)} - 2\bar{m}_{11}D_0\sigma_0\right. \\ & \left.\left.\left. + \ \ \bar{m}_{12}\varepsilon^{(c)}\sigma_0\right)\right)\right), \end{aligned} \tag{A.8}$$

$$\begin{aligned} a_2 = {} & -2\bar{m}_{21}^2\bar{m}_{32}D_0\varepsilon^{(c)} + \bar{m}_{31}\mu^{(c)}\left(\bar{m}_{23}\bar{m}_{31}D_0 - 2\bar{m}_{23}\bar{m}_{32}\varepsilon^{(c)}\right. \\ & \left. + \bar{m}_{13}\bar{m}_{31}\sigma_0 - \bar{m}_{11}\bar{m}_{33}\sigma_0\right) - \bar{m}_{22}^2\bar{m}_{31}\varepsilon^{(c)2} \\ & + \bar{m}_{21}\left(-\bar{m}_{31}\bar{m}_{32}B_0\varepsilon^{(c)} - \bar{m}_{31}\bar{m}_{33}D_0\mu^{(c)}\right. \\ & \left. + \bar{m}_{32}\bar{m}_{33}\varepsilon^{(c)}\mu^{(c)}\ \bar{m}_{12}\bar{m}_{31}\varepsilon^{(c)}\sigma_0 - 2\bar{m}_{11}\bar{m}_{32}\varepsilon^{(c)}\sigma_0\right) \\ & + \bar{m}_{22}\varepsilon^{(c)}\left(\bar{m}_{31}^2B_0 + \bar{m}_{21}\bar{m}_{32}\varepsilon^{(c)}\right. \\ & \left. + \ \bar{m}_{31}\left(2\bar{m}_{21}D_0 + \bar{m}_{33}\mu^{(c)} + \bar{m}_{11}\sigma_0\right)\right), \end{aligned} \tag{A.9}$$

$$\begin{aligned} a_3 = {} & -\bar{m}_{21}\bar{m}_{22}\bar{m}_{31}\varepsilon^{(c)} + \bar{m}_{21}^2\bar{m}_{32}\varepsilon^{(c)} - \bar{m}_{23}\bar{m}_{31}^2\mu^{(c)} \\ & + \bar{m}_{21}\bar{m}_{31}\bar{m}_{33}\mu^{(c)}. \end{aligned} \tag{A.10}$$

References

Avellaneda M, Harshe G (1994) Magnetoelectric effect in piezoelectric/magnetostrictive multiplayer (2-2) composites. J Intell Mater Syst Struct 5:501–513

Benveniste Y (1995) Magnetoelectric effect in fibrous composites with piezoelectric and piexomagnetic phases. Phys Rev B 51:16424–16427

Chen WQ, Shioya T (1999) Fundamental solution for a penny-shaped crack in a piezoelectric medium. J Mech Phys Solids 47:1459–1475

Chue CH, Liu TJC (2005) Magneto-electro-elastic antiplane analysis of a biomaterial $BaTiO_3$–$CoFe_2O_4$ composite wedge with an interface crack. Theor Appl Fract Mech 44:275–296

Dunn ML (1994) The effects of crack face boundary conditions on the fracture mechanics of piezoelectric solids. Eng Fract Mech 48:25–39

Feng WJ, Su RKL (2006) Dynamic internal crack problem of a functionally graded magneto-electro-elastic strip. Int J Solids Struct 43:5196–5216

Feng WJ, Xue Y, Zou ZZ (2005) Crack growth of an interface crack between two dissimilar magneto-electro-elastic materials under anti-plane mechanical and in-plane electric magnetic impact. Theor Appl Fract Mech 43:376–394

Feng WJ, Pan E, Wang X (2007) Dynamic fracture analysis of a penny-shaped crack in a magnetoelectroelastic layer. Int J Solids Struct 44:7944–7955

Gao CF, Fan WX (1999) Exact solutions for the plane problem in piezoelectric materials with an elliptic or a crack. Int J Solids Struct 36:2527–2540

Gao CF, Noda N (2004) Thermal-induced interfacial cracking of magnetoelectroelastic materials. Int J Eng Sci 42:1347–1360

Gao CF, Tong P, Zhang TY (2003) Interfacial crack problems in magneto-electroelastic solids. Int J Eng Sci 41:2105–2121

Hao TH, Shen ZY (1994) A new electric boundary condition of electric fracture mechanics and its applications. Eng Fract Mech 47:793–802

Harshe G, Dougherty JP, Newnham RE (1993) Theoretical modeling of 3-0/0-3 magnetoelectric composites. Int J Appl Electromagn Mech 4:161–171

Hu KQ, Li GQ (2005) Electro-magneto-elastic analysis of a piezoelectromagnetic strip with a finite crack under longitudinal shear. Mech Mater 37:925–934

Hu KQ, Kang YL, Li GQ (2006) Moving crack at the interface between two dissimilar magnetoelectroelastic materials. Acta Mech 182:1–16

Huang JH, Kuo WS (1997) The analysis of piezoelectric/piezomagnetic composite materials containing an ellipsoidal inhomogeneity. J Appl Phys 81:1378–1386

Jiang LZ, Sun CT (2001) Analysis of indentation cracking in piezoceramics. Int J Solids Struct 38:1903–1918

Karapetian E, Sevostianov I, Kachanov M (2000) Penny-shaped and half-plane cracks in a transversely isotropic piezoelectric solid under arbitrary loading. Arch Appl Mech 70:201–229

Kirchner HOK, Alshits I (1996) Elastically anisotropic angularly inhomogeneous media II. The Green's function for piezoelectric, piezomagnetic and magnetoelectric media. Philos Mag A 74:861–885

Kogan L, Hui CY, Molcov V (1996) Stress and induction eld of a spheroidal inclusion of a penny-shaped crack in a transversely isotropic piezoelectric material. Int J Solids Struct 33:2719–2737

Li JY, Dunn ML (1998) Micromechanics of magneto-electro-elastic composite materials: average fields and effective behavior. J Intell Mater Syst Struct 9:404–416

Li R, Kardomateas GA (2006) The Mode III interface crack in piezo-electro-magneto-elastic dissimilar bimaterials. J Appl Mech 73:220–227

Li XF, Lee KY (2004) Effects of electric field on crack growth for a penny-shaped dielectric crack in a piezoelectric layer. J Mech Phys Solids 42:2079–2100

Liu JX, Liu X, Zhao Y (2001) Explicit expressions of the generalized Barnett–Lothe tensors for anisotropic piezoelectric materials. Int J Eng Sci 39:1803–1814

McMeeking RM (1999) Crack tip energy release rate for a piezoelectric compact tension specimen. Eng Fract Mech 64:217–244

McMeeking RM (2001) Towards a fracture mechanics for brittle piezoelectric and dielectric materials. Int J Fract 108:25–41

Nan CW (1994) Magneto-electric effect in composites of piezoelectric and piezomagnetic phases. Phys Rev B 50:6082–6088

Niraula OP, Wang BL (2006) A magneto-electro-elastic material with a penny-shaped crack subjected to temperature loading. Acta Mech 187:151–168

Pak YE (1990) Crack extension force in a piezoelectric material. J Appl Mech 57: 647–653

Pak YE (1992) Linear electroelastic fracture mechanics of piezoelectric materials. Int J Fract 54:79–100

Park S, Sun CT (1995) Fracture criteria for piezoelectric ceramics. J Am Ceram Soc 78:1475–1480

Parton VZ (1976) Fracture mechanics of piezoelectric materials. Acta Astron 3:671–683

Song ZF, Sih GC (2003) Crack initiation behavior in magneto-electroelastic composite under in-plane deformation. Theor Appl Fract Mech 39:189–207

Sosa H, Khutoryansky N (1996) New developments concerning piezoelectric materials with defects. Int J Solids Struct 33:3399–3414

Tian WY, Gabbert U (2005) Macrocrack–microcrack interaction problem in magnetoelectroelastic solids. Mech Mater 37:565–592

Wang B (1992) Three-dimensional analysis of a flat elliptical crack in a piezoelectric material. Int J Eng Sci 30:781–791

Wang XD, Jiang LY (2002) Fracture behavior of cracks in piezoelectric media with electromechanically coupled boundary conditions. Proc R Soc Lond Ser A458:2545–2560

Wang XD, Jiang LY (2004) The nonlinear fracture behavior of an arbitrary originated dielectric crack in piezoelectric materials. Acta Mech 172:195–210

Wang BL, Mai YW (2003) On the electrical boundary conditions on the crack surfaces in piezoelectric ceramics. Int J Eng Sci 41:633–652

Wang BL, Mai YW (2004) Fracture of piezoelectromagnetic materials. Mech Res Commun 31:65–73

Wang BL, Mai YW (2007) Applicability of the crack-face electromagnetic boundary conditions for fracture of magneto-electroelastic materials. Int J Solids Struct 44:387–398

Xu XL, Rajapakse RKND (2001) On a plane crack in piezoelectric solids. Int J Solids Struct 38:7643–7658

Yang JH, Lee KY (2002) Three-dimensional non-axisymmetric behavior of a penny-shaped crack in a piezoelectric strip

subjected to in-plane loads. Eur J Mech A/Solids 21:223–237

Yang JH, Lee KY (2003) Penny shaped crack in a piezoelectric cylinder surrounded by an elastic medium subjected to combined in-plane mechanical and electrical loads. Int J Solids Struct 40:573–590

Zhang TY, Qian CF, Tong P (1998) Linear electroelastic analysis of a cavity or a crack in a piezoelectric material. Int J Solids Struct 35:2121–2149

Zhang TY, Zhao MH, Tong P (2002) Fracture of piezoelectric ceramics. Adv Appl Mech 38:147–289

Zhao MH, Yang F, Liu T (2006) Analysis of a penny-shaped crack in a magneto-electro-elastic medium. Philos Mag 86:4397–4416

Zhou ZG, Wang B, Sun YG (2004) Two collinear interface cracks in magneto-electro-elastic composites. Int J Eng Sci 42:1155–1167